

Predicting the high temperature effect on mortar compressive strength by neural network

N. Yuzer¹, B. Akbas² and A.B. Kizilkanat*¹

¹*Yildiz Technical University, Department of Civil Engineering, Istanbul 34210, Turkey*

²*Gebze Institute of Technology, Kocaeli, Turkey*

(Received February 24, 2010, Revised June 28, 2010, Accepted January 20, 2011)

Abstract. Before deciding if structures exposed to high temperature are to be repaired or demolished, their final state should be carefully examined. Destructive and non-destructive testing methods are generally applied for this purpose. Compressive strength and color change in mortars are observed as a result of the effects of high temperature. In this study, ordinary and pozzolan-added mortar samples were produced using different aggregates, and exposed to 100, 200, 300, 600, 900 and 1200°C. The samples were divided into two groups and cooled to room temperature in water and air separately. Compression tests were carried out on these samples, and the color change was evaluated by the Munsell Color System. The relationships between the change in compressive strength and color of mortars were determined by using a multi-layered feed-forward Neural Network model trained with the back-propagation algorithm. The results showed that providing accurate estimates of compressive strength by using the color components and ultrasonic pulse velocity design parameters were possible using the approach adopted in this study.

Keywords: color; concrete; high temperature; neural network; pulse velocity; strength.

1. Introduction

At elevated temperatures, a change in the concrete color may be observed, especially when the river siliceous aggregate is used. For example, previous studies have reported that pink or red colors on the concrete surface indicated that the concrete had been exposed to a temperature of about 300-600°C. The gray color, however, shows that the concrete has suffered a temperature ranging from 600°C to 900°C. Moreover, the compressive strength of the concrete decreases about 50% when the temperature reaches to 600°C. This fact justifies that residual strength of the concrete can be predicted after being subjected to elevated temperature by observing the color change (Neville 2000). Furthermore, Wang (2008) reported that variation in color on the surface may help estimate the highest elevated temperatures that concrete structures can withstand.

Color is one of the physical properties of a material assessed by various color systems. The Munsell Color System evaluates the color change quantified by decimal numbers considering the components of hue, lightness, and chroma degree of the color (Fig. 1). The first component, hue, indicates the color different from the other colors. The Munsell Color System describes the hue with the numbers between 1 and 100 in a circular segment (Fig. 2). In the circular segment, red 5 (5R), yellow 25 (5Y), green 45 (5G), blue 65 (5B), and purple 85 (5P) are placed sequentially occupying

* Corresponding author, E-mail: bkkanat@yildiz.edu.tr

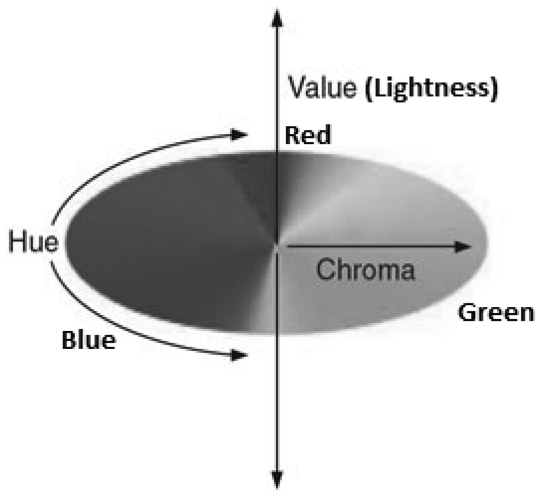


Fig. 1 Dimensions of the surface-color-perception solid

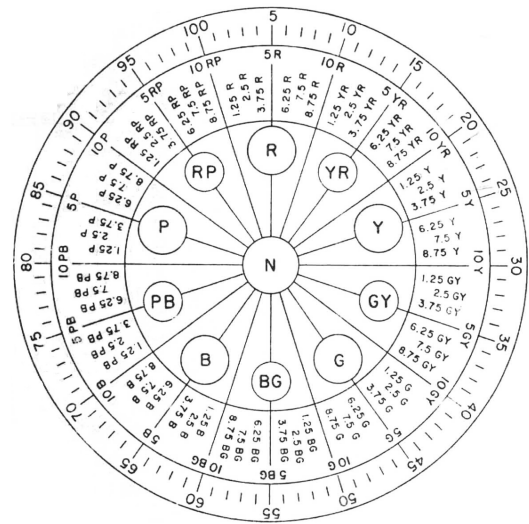


Fig. 2 Designation systems for Munsell hue

5 equal segments. Similarly, the mixtures of these colors such as yellow-red 15 (5YR), green-yellow 35 (5GY), blue-green 55 (5BG), purple-blue 75 (5PB), and red-purple 95 (5RP) are placed in the circle (Fig. 2). Thus, ten segments are subdivided into ten equal parts for generating the decimal number system. The second component lightness, on the other hand, describes the brightness of the color and is designated with numbers 0 to 10. In this scale, 0 and 10 stand for black and white, respectively. Degree of chroma is a component to identify a color. This indicates the amount of gray in the color through the numbers 0 to 20. The chroma points out degree of departure of a color from gray (Luke 1996, ASTM D 1535-08).

An experimental study was performed to investigate the effect of high temperature on mortars, with and without pozzolan, by using the Munsell color measuring system according to ASTM D 1535-08. The compressive strength and the corresponding color change of each mortar specimen, subjected to different temperature levels, were evaluated and a meaningful relationship between them was found in a previous study by Yuzer and Kizilkanat (2008). In another research by Short *et al.* (2001), the compressive strength and color change of the concrete exposed to high temperature were measured. It was found that there was a good relation between these two parameters for the concretes made with siliceous aggregates. An experimental study carried out by Lou and Lin (2007) states that the intensity of red color on the mortar surface rises when exposed to high temperature. The effects of high temperatures on mortar were analyzed using Energy Dispersive Signals. The composition analyzed after fire, and the variations of Si, O and Ca were determined. As a result we can say that there is a correlation between surface color and the minerals of components of the mortar at elevated temperatures. Consequently, the evaluation of the surface color of the concrete structures exposed to fire may be used for predicting the residual compressive strength.

Advances in computer and software technology have enabled the use of Neural Network (NN) analysis for establishing non-linear relationships in engineering problems. NN analysis offers more realistic and accurate predictions. A NN model is designed based on simulating the structure and learning activities of the human brain. Garrett *et al.* (1997) defines a NN model as a computational

mechanism able to acquire, represent, and compute mapping from one multivariate space of information to another, given a set of data representing that mapping.

NN has been widely used in structural engineering for almost the last two decades (Flood 1989, Zhao 2006, Yuzer *et al.* 2007) because most of the structural engineering problems are often too complicated and include incomplete and noisy data. The most recent studies include predicting the compressive strength of concrete using neural networks. Bilim *et al.* (2009) studied applicability of neural network models on predicting the compressive strength of granulated blast furnace slag concrete. They used different water-cement ratios, cement dosages and slag replacement ratios in their NN models consisting of different algorithms. Their findings show that NN models can be an alternative method for estimating the compressive strength of ground granulated blast furnace slag concrete. Saridemir (2009) also used NN models to predict the compressive strength of concrete containing metakaolin and silica fume. He suggested that estimating compressive strength of concretes containing metakaolin and silicafume with NN models save time and money. Parichatprecha and Nimityongskul (2009) tried to predict the high performance concrete by NN models. They used water and cement, water-binder ratio, fly ash and silica fume as variables in their study. Their model resulted with an absolute fraction of variance (R^2) of 99%. In another research (Chiang and Yang 2005) which utilized Neural Network applications in order to predict residual compressive strength due to high temperature, it was emphasized that maximum exposure temperature, exposure time and heating and cooling rates were the most important factors. In the study, exposure time, exposure temperature, water/cement ratio and residual pulse velocity were chosen as input parameters. Good agreement was observed between the predicted residual strength and the target values of compressive strength.

2. Research significance

Many methods have been developed to determine concrete quality. Sonreb Method is one of these methods and which uses results of ultrasonic pulse velocity and rebound tests (Akman and Guner 1984). However this method does not perfectly give us accurate result of concrete quality. Since carbonation of concrete that is exposed to high temperature is higher than the concrete that not exposed to. This is because carbonation increases surface hardness value so this situation misleads the determination of concrete quality. Therefore in our study to get more accurate results for determining quality of concrete that exposed high temperature, in addition to ultrasonic pulse velocity, color components were used instead of surface hardness. The principal aim of this study is to develop and test multi-layered feedforward NNs, trained with the back-propagation algorithm, to model the non-linear relationship among the three components of color, ultrasonic pulse velocity and the compressive strength of concrete. To determine the above-mentioned input parameters, an experimental program was carried out. First, eight series mortar specimens made of different aggregates and mineral admixtures were exposed to high temperature effect. Then a relationship was established using Neural Network analysis with these parameters, such as the change in color, ultrasonic pulse velocity, and compressive strength. By using the NN model developed in this study, an engineer can predict the compressive strength of the concrete with a very high accuracy.

3. Experimental procedure

The experimental study consisted of four parts, namely production of mortar specimens, curing, heating and cooling duration, and physical and mechanical control testing.

3.1 Materials and specimen preparation

The mortar production was made with standard CEN sand and calcareous aggregates with the same granulometry, ordinary Portland cement (CEM I 42.5 R), microsilica, fly ash, and slag. The properties of cement and mineral admixtures are given in Table 1. Mineral admixtures replaced 10 % cement by weight. The water-cementitious material ratio was kept at 0.50, and the workability adjusted by using superplasticizer at required dosage (0.4-2%). A total of 336 prism specimens with dimensions of 40×40×160 mm were prepared. Three specimens were used for each temperature

Table 1 Chemical and physical properties of portland cement and mineral admixtures

Chemical composition (%)	Portland cement	Microsilica	Fly ash	B.F. Slag
CaO	64.01	0.57	8.72	33.48
SiO ₂	20.01	82.22	57.27	41.43
Al ₂ O ₃	5.28	0.17	14.15	10.28
Fe ₂ O ₃	3.65	0.53	12.52	3.48
MgO	1.21	5.43	1.33	6.05
SO ₃	2.47	1.42	0.56	-
Loss on ignition	2.27	3.96	-	0.61
Specific weight (g/cm ³)	3.14	2.02	2.01	2.80
Specific surface (Blaine, cm ² /g)	3570	---	3621	3910

Table 2 Specimen code

Cooling type	In air (A)		In water (W)	
	Siliceous (S)	Limestone (L)	Siliceous (S)	Limestone (L)
Type of pozzolan				
Ordinary portland cement (O)	OSA	OLA	OSW	OLW
Microsilica (Ms)	MsSA	MsLA	MsSW	MsLW
Fly ash (F)	FSA	FLA	FSW	FLW
Blast furnace slag (B)	BSA	BLA	BSW	BLW

Table 3 Mix proportions of mortar specimens (kg/m³)

Series	OS	MsS	FS	BS	OL	MsL	FL	BL
Cement	508	446	451	458	517	458	459	461
W/C	0.5	0.5	0.5	0.5	0.5	0.5	0.5	0.5
Fine aggregate	1525	1484	1501	1524	1552	1527	1529	1537
Silica fume	-	49	-	-	-	51	-	-
Fly ash	-	-	50	-	-	-	51	-
Slag	-	-	-	50	-	-	-	51
Superplasticizier (%)	0.5	0.4	0.4	0.4	1.7	2	2	2

level. Prism mortar specimens conforming to TS EN 196-1 (2002) were demolded after 24 hours and then stored in water tank at $20\pm 2^\circ\text{C}$ until the testing day. The testing specimens were coded according to aggregate type, mineral admixture, and the cooling method, and are shown in Table 2. For example, MsLA means that silica fume added mortar has been mixed with limestone aggregate and cooled in air to the room temperature. The mix proportions are summarized in Table 3.

3.2 High temperature effect and control tests

Heating and cooling procedures were planned as follows: specimens were heated to specified temperature level without loading, then cooled to room temperature, and then tested. After 28 days of curing period, specimens were dried in oven at $100\pm 5^\circ\text{C}$ for 48 hours. Thereafter, the three specimens of each group were heated up to 100, 200, 300, 600, 900 and 1200°C with $6\text{-}10^\circ\text{C}$ per minute heating rate furnace (Fig. 3). After the target temperature was reached, all the samples were removed from the furnace. Two cooling regimes were chosen. In one of the regimes, the specimens were allowed to cool naturally to the room temperature ($20\pm 2^\circ\text{C}$) (Fig. 4). The other was rapid cooling, the heated specimens were taken out of the furnace and immersed in water tank and then



Fig. 3 Specimens heated up to 1200°C in the furnace



Fig. 4 Specimens after exposed to 1200°C

Table 4 Design parameters

Design parameter	Definition	Range
X_1	Hue (1-100)	17.6-27.6
X_2	Lightness (0-10)	3.8-7.6
X_3	Chroma (0-20)	0.2-2.9
X_4	Pulse velocity ($\text{mm}/\mu\text{sec}$)	0.59-4.3
Y	Compressive strength (N/mm^2)	2.8-60.0

Table 5 Test results of the control specimens (20°C)

Specimen	Hue	Lightness	Chroma	Pulse velocity (mm/ μ s)	Compressive strength (N/mm ²)
OS	25.8	7.2	0.5	3.93	44.2
MsS	26.4	6.2	0.4	4.27	56.6
BS	22.7	6.5	0.8	3.94	48.3
FS	24.3	6.7	0.5	3.85	45.8
OL	27.9	6.3	0.4	3.96	50.8
MsL	27.3	6.1	0.6	4.26	54.2
BL	25.6	6.3	0.5	3.97	54.8
FL	26.2	6.4	0.5	3.87	57.7

Table 6 Cases used in constructing the NN model

Case No.	Specimen code	(X_1)	(X_2)	(X_3)	(X_4)	(Y_1)	(Y_{NN})
1	OSW-100°C	25.7	7.0	0.5	4.08	48.5	50.06
2	OSW-300°C	23.2	6.5	0.8	3.72	33.5	39.05
3	OSA-600°C	19.7	6.5	0.7	3.22	41.8	53.59
4	OSW-600°C	20.9	5.4	1.1	3.19	30.4	32.61
5	OSA-900°C	18.9	7.6	0.4	1.31	20.5	19.87
6	OSA-1200°C	23.2	7.5	1.1	0.93	4.6	5.01
7	MsS-20°C	26.4	6.2	0.4	4.27	56.6	53.13
8	MsSA-100°C	26.8	6.3	0.4	4.09	51.3	52.58
9	MsSW-100°C	26.6	6.3	0.4	4.17	59.8	52.83
10	MsSA-200°C	27.2	6.0	0.4	4.15	49.5	52.91
11	MsSW-200°C	25.4	5.9	0.4	4.19	51.1	53.31
12	MsSA-300°C	25.6	5.9	0.5	4.06	57.3	52.48
13	MsSA-600°C	21.5	5.6	0.9	3.42	21.9	33.65
14	MsSW-600°C	22.0	4.2	0.9	3.24	39.0	38.10
15	MsSA-900°C	22.5	6.5	1.0	1.33	15.6	14.01
16	MsSW-900°C	21.6	4.6	1.3	1.36	11.5	13.73
17	MsSA-1200°C	20.1	6.7	2.9	0.96	3.1	3.01
18	MsSW-1200°C	20.7	5.6	2.6	1.20	2.8	3.02
19	BS-20°C	22.7	6.5	0.8	3.94	48.3	49.47
20	BSA-100°C	22.5	6.8	0.7	3.83	50.0	45.60
21	BSA-200°C	22.3	6.5	0.7	3.92	54.2	49.08
22	BSA-300°C	22.1	6.3	0.9	3.89	58.8	51.48
23	BSW-300°C	22.4	5.5	1.1	3.72	47.9	44.24
24	BSA-600°C	19.6	5.3	1.5	3.23	51.9	52.38
25	BSW-600°C	19.8	4.0	1.2	3.04	29.4	27.75
26	BSA-900°C	17.6	6.6	0.8	1.20	17.9	19.15
27	BSW-900°C	18.6	4.5	1.4	1.45	7.9	8.36
28	BSA-1200°C	20.1	6.7	1.5	0.59	6.0	6.24
29	BSW-1200°C	19.6	5.3	2.0	0.84	4.1	3.10
30	FSA-100°C	22.3	6.7	0.4	4.01	49.2	48.65

Table 6 Continued

Case No.	Specimen code	(X_1)	(X_2)	(X_3)	(X_4)	(Y_i)	(Y_{NN})
31	FSA-200°C	22.3	6.6	0.5	3.94	44.4	47.34
32	FSW-200°C	22.4	6.8	0.5	3.82	36.9	42.08
33	FSW-300°C	22.5	6.6	0.8	3.67	33.5	39.98
34	FSA-600°C	20.8	5.4	1.4	3.42	50.4	47.71
35	FSW-600°C	21.2	5.0	1.2	3.45	30.0	37.52
36	FSA-900°C	20.0	6.8	0.4	1.33	13.0	16.63
37	FSW-900°C	19.7	4.6	1.0	1.62	22.9	18.53
38	FSA-1200°C	20.3	6.9	1.9	0.90	6.5	6.22
39	FSW-1200°C	19.4	5.4	2.6	1.50	4.4	3.55
40	OL-20°C	27.9	6.3	0.4	3.96	50.8	52.03
41	OLA-100°C	29.5	6.6	0.3	3.79	49.9	51.32
42	OLW-100°C	31.0	6.6	0.2	3.81	51.3	52.05
43	OLA-200°C	28.9	6.9	0.2	3.81	55.4	51.09
44	OLW-200°C	28.9	6.5	0.3	3.81	47.5	51.57
45	OLA-300°C	28.7	6.9	0.3	3.79	45.7	50.07
46	OLA-600°C	19.8	6.6	0.8	2.83	53.1	51.80
47	OLW-600°C	20.2	6.0	0.7	2.72	32.5	32.35
48	OLA-900°C	21.3	6.9	0.7	2.50	35.8	33.21
49	OLW-900°C	20.3	5.0	1.1	2.52	24.4	23.97
50	OLA-1200°C	24.3	7.6	1.5	1.60	5.2	6.52
51	MsL-20°C	27.3	6.1	0.6	4.26	54.2	51.54
52	MsLA-100°C	28.6	6.1	0.3	4.30	58.1	53.10
53	MsLW-100°C	29.5	6.2	0.3	4.19	58.5	52.71
54	MsLA-200°C	30.1	6.1	0.2	4.26	51.7	53.11
55	MsLW-200°C	29.4	6.1	0.3	4.29	48.8	52.82
56	MsLA-300°C	25.6	5.7	0.5	4.23	49.2	53.06
57	MsLA-600°C	19.6	6.1	0.7	3.77	60.0	57.26
58	MsLW-900°C	19.9	5.3	1.3	1.85	24.4	17.53
59	BL-20°C	25.6	6.3	0.5	3.97	54.8	51.08
60	BLA-100°C	24.7	6.7	0.4	3.71	57.1	40.90
61	BLW-100°C	25.5	6.0	0.4	4.02	54.0	52.59
62	BLA-200°C	24.6	6.5	0.4	4.01	50.2	50.69
63	BLW-200°C	25.5	5.9	0.4	4.00	50.0	52.65
64	BLW-300°C	24.8	5.9	0.5	3.74	39.4	48.59
65	BLA-600°C	19.5	5.7	1.1	3.28	54.8	54.15
66	BLA-900°C	18.3	6.6	1.1	2.50	42.5	40.82
67	BLW-900°C	18.8	4.8	1.4	2.32	29.2	33.20
68	BLA-1200°C	22.7	6.8	2.2	1.39	4.2	3.23
69	FL-20°C	26.2	6.4	0.5	3.87	57.7	49.88
70	FLA-100°C	27.9	6.7	0.3	4.00	56.3	52.17
71	FLW-100°C	26.2	6.1	0.4	4.02	52.1	52.54
72	FLA-200°C	26.5	6.7	0.3	4.06	46.0	52.19
73	FLW-200°C	26.8	6.7	0.3	4.00	46.0	51.85
74	FLW-300°C	25.9	6.4	0.3	3.73	39.0	48.06

Table 6 Continued

Case No.	Specimen code	(X_1)	(X_2)	(X_3)	(X_4)	(Y_1)	(Y_{NN})
75	FLA-600°C	20.0	6.1	0.9	3.08	57.7	48.53
76	FLW-600°C	20.8	5.0	1.0	3.38	45.6	35.08
77	FLW-900°C	19.7	5.6	1.5	2.25	29.0	31.47
1	OS-20°C	25.8	7.2	0.5	3.93	44.2	45.76
2	OSA-100°C	25.1	7.2	0.6	3.95	45.0	44.55
3	OSA-200°C	24.6	7.1	0.5	3.89	44.4	43.07
4	OSW-200°C	24.6	6.7	0.6	3.93	42.6	46.96
5	OSA-300°C	22.1	7.0	1.0	3.82	43.4	56.18
6	MsSW-300°C	24.0	5.5	0.6	4.01	46.3	52.28
7	BSW-100°C	22.6	6.8	0.7	3.88	47.8	47.04
8	BSW-200°C	22.6	6.0	0.8	3.78	45.8	44.58
9	FS-20°C	24.3	6.7	0.5	3.85	45.8	44.60
10	FSW-100°C	23.7	6.1	0.5	3.94	47.3	50.06
11	FSA-300°C	22.7	6.4	0.6	3.88	40.7	45.99
12	OLW-300°C	27.6	6.2	0.2	3.82	44.2	52.38
13	MsLW-300°C	26.7	6.4	0.4	4.15	48.1	52.67
14	MsLW-600°C	18.7	3.8	0.4	3.71	40.6	51.00
15	MsLA-900°C	20.8	7.4	0.6	2.30	43.1	41.07
16	BLA-300°C	25.1	6.6	0.4	3.67	42.9	41.60
17	BLW-600°C	20.2	4.8	1.0	3.52	41.3	43.20
18	FLA-300°C	25.7	6.6	0.4	3.69	43.5	44.05
19	FLA-900°C	19.6	6.9	1.0	2.48	41.3	48.28

cooled to room temperature. After this process, the samples were kept 24 ± 1 hours under the laboratory conditions so that the surface of the samples became dry.

After heating and cooling, the color components of the specimens were measured using spectro photometer, ultrasonic pulse velocities were obtained and compressive strength tests carried out finally. Design parameters and test results are given in Table 4-6.

4. Neural network design

Neural networks (NNs) are considered to be simple mathematical structures and suitable tools in establishing a reliable non-linear relationship among the various parameters. No complex mathematical formulations are needed to design a NN. A NN model can be defined using three basic components: transfer function, network architecture, and the learning law. NN models learn and generalize from examples and experience to produce meaningful solutions to the problems even in cases where the input data contains error or is incomplete (Rafiq *et al.* 2001, Gunaydin and Dogan 2004). The three-layer feedforward NN model with 4 input nodes, 1 hidden layer and one output node is shown in Fig. 5. The data presented to the NN model are represented by the input nodes, whereas the outputs of the NN model are represented by the output nodes.

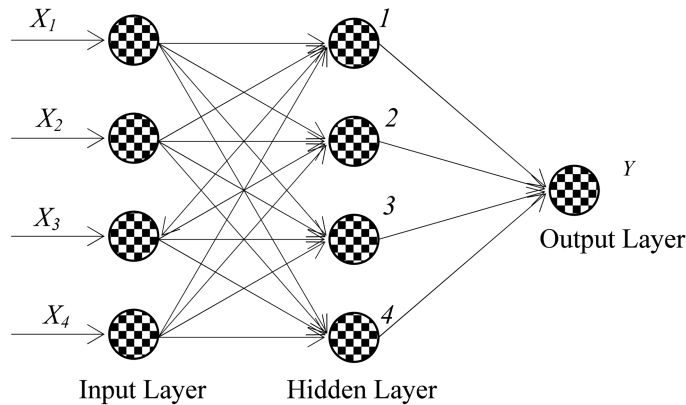


Fig. 5 Neural network model

A typical NN model consists of a group of processing elements (PEs), or neurons, linked together for constructing a relation in an input/output set of learning patterns. A PE is an information-processing unit with three basic components: (1) a set of synapses; (2) an adder; (3) an activation function. It may be defined by computing the sum of their weighted inputs, subtracting its threshold from the sum, and transferring these results by a function as follows (Haykin 1994)

$$u_i = \left(\varphi \sum_{j=1}^n w_{ij} x_j - \theta_i \right) \quad (1)$$

where u_i represents the output of a PE, w_{ij} represents the synaptic weights associated with PE i , x_j represents the input signal, θ_i represents the threshold value of the PE, and $\varphi(\cdot)$ presents the activation (or transformation) function. Any change in the synaptic weights will, in turn, change the input-output behavior of the NN model (Haykin 1994). The most common form of activation function used in the construction of NN model is the hyperbolic tangent function which generates output values between -1 and 1 as given below (Neuro Solutions 2003)

$$f(x_i) = \tanh(\beta x_i) \quad (2)$$

where β controls the slope of the function. It is generally recommended to carry out a parametric study by changing the number of PEs in the hidden layer in order to test the stability of the network (Neuro Solutions 2003). In many engineering problems, a single hidden layer with an optimum number of PEs is considered to be sufficient (Rafiq *et al.* 2001).

Supervised and unsupervised learning algorithms are the two classes of NN model. Supervised learning NN algorithms, for example back propagation neural networks (BPNNs), require the training data to have been previously specified in different classes so that a subsequent test sample may be assigned to the most appropriate class. Even though they train slowly and require many training data, BPNN is the most commonly used NN algorithm for the analysis of structural and civil engineering problems due to its versatile and robust technique and are capable of solving predictive problems (Neuro Solutions 2003). Training data need not be specified in unsupervised learning, since it organizes the data into clusters for the purpose of defining the various similarities that exist within the data set. Test data is then examined to check if it falls within any of the clusters in the training data (Yeung and Smith 2005). In this study, supervised learning algorithms

with static back-propagation neural network are selected.

The NN model in this study was developed in three steps: the modeling, the training, and the testing steps. The experimental study, the identification of changes in color and ultrasonic pulse velocity, and the internal rules were considered in the modeling phase. The preparation of the data and the adaptation of the learning law for the training were performed during the training phase. And the prediction accuracy of the model was evaluated at the testing phase, i.e. the comparison of the actual and estimated compressive strengths.

4.1 Modeling the neural network

The selection of the input variables affects the accuracy of the NN model predictions significantly. In this study, the variables hue, lightness, chroma and pulse velocity were considered for the input layer to evaluate the compression strength (output data) as shown in Table 4. The parameters are 1) X1, 2) X2, 3) X3, 4) X4. Parameter 1 is the hue, parameter 2 is the lightness, parameter 3 is the chroma, and parameter 4 is the pulse velocity. The ranges of data for the selected design variables are given in Table 4. All the design variables were input to the NN as given above.

A total of 96 cases were used for the NN model. Table 6 shows the value of the design parameters for each case. The compression strength (output) and the input variables from the 96 cases were divided into two sets. One set was put aside for the training of the NN (first 77 cases in Table 6), and the other was for validating the performance of the trained network (testing). For testing purposes, 20% of the 96 cases (19 cases) were selected at random order for the testing set for each training cycle (cases below the dotted line in Table 6). The data between the maximum and minimum were selected for testing purposes. The data set including training and testing was first normalized for the NN model.

4.3 The training step

The standard back-propagation (BP) algorithm for the training of the network was employed in this study using a commercial NN software (Neuro Solutions 2003). The NN models were created using an input layer of 4 PEs corresponding to the 4-input parameters, and one PE corresponding to an output layer selected as the target (Fig. 5). Several trials during the testing phase led to the selection of one hidden layer and the hyperbolic tangent function was used as the activation function.

In BP algorithm, NN models learn from examples and training or learning data are introduced into the network with a series of examples of associated input and target output values. During the learning, a gradual reduction of error between the model output and the target output occurs, and the error is evaluated using the mean square error (MSE) as follows (Gunaydin and Dogan 2004, Haykin 1994)

$$MSE = \sqrt{\frac{\sum_{i=1}^n (y_i - Y(i))^2}{n}} \quad (3)$$

where n is the number of samples to be evaluated in the training phase, ($n = 77$ for this study), y_i is the model output related to the sample i ($i = 1, 2, \dots, n$), and $Y(i)$ is the target output, i.e. the

estimated compression strength. MSE is a good indicator of how successful the training run was. The error was measured for each run of the epoch number selected. Epoch number shows the training of all cases in a training set. Training is stopped when the MSE remained unchanged for a given number of epochs. If it is not stopped, the NN memorizes the training values, and is unable to make predictions when an unknown example is introduced to the NN. For supervised learning control, the maximum number of epochs should be specified showing the number of iterations over the training set. In this study, an epoch number of 6500 was found to be adequate for the final training process in a series of more than 250 runs for the NN model.

Each layer in NN model has a vector of *PEs*, learning rule, and learning parameters. The learning rule is the way by which the correction term is introduced. The learning rate is the amount of correction to be applied to the weights. Momentum as the learning rule is widely used due to its simplicity and efficiency compared to the standard gradient minimum. The appropriate step size and learning rate (momentum coefficient) should be decided based on the learning of the network. These terms are specified at the start of the training cycle and affect the speed and stability of the NN. The learning rate ranges between 0.0-1.0 and determines the amount of weight modification among the neurons during each cycle of training iteration (Neuro Solutions 2003). In this study, a momentum coefficient of 0.1 for the hidden layer, and 0.7 for the output layer functioned very well, therefore, the step size was selected as 1.0 for the hidden layer and 0.7 for the output layer.

4.4 The testing step

Testing set shows the performance of the NN model. The testing is performed with the best weights obtained during the training. The weighting factors remain unchanged in this phase. The trained weighting factors of the NN are validated with testing data to test the accuracy of the predictions of the trained NN model. The NN's performance in this study, for both training and testing cases, was measured by using the absolute compressive strength percentage error (*EPE_{CS}*) formula as follows

$$EPE_{CS} = \left| \frac{y(i) - Y(i)}{Y(i)} \right| \times 100\% \quad (4)$$

Overall performance of the NN model may be evaluated through weighted error (*WE*) which can be defined as follows (Hegazy 1998)

$$WE(\%) = 0.5(\text{Average } EPE_{CS} \text{ for Training Set} + \text{Average } EPE_{CS} \text{ for Testing Set}) \quad (5)$$

5. Discussion

Test results have shown that high temperature caused significant variation in strength, ultrasonic pulse velocity and color of mortar (Table 6). The use of mineral admixture, aggregate type, and cooling method were influential on this variation. These variations were observed; compressive strength and ultrasonic pulse velocity were decreased meanwhile color of mortar turned from yellow to red (Figs. 6-15). Samples cooled in water have shown less compressive strength than samples cooled in air (Figs. 6 and 7). This is because huge thermal stress and cracks could happen if the variation of temperature is fast and the temperature gradient is high (Shackelford 2005). In addition,

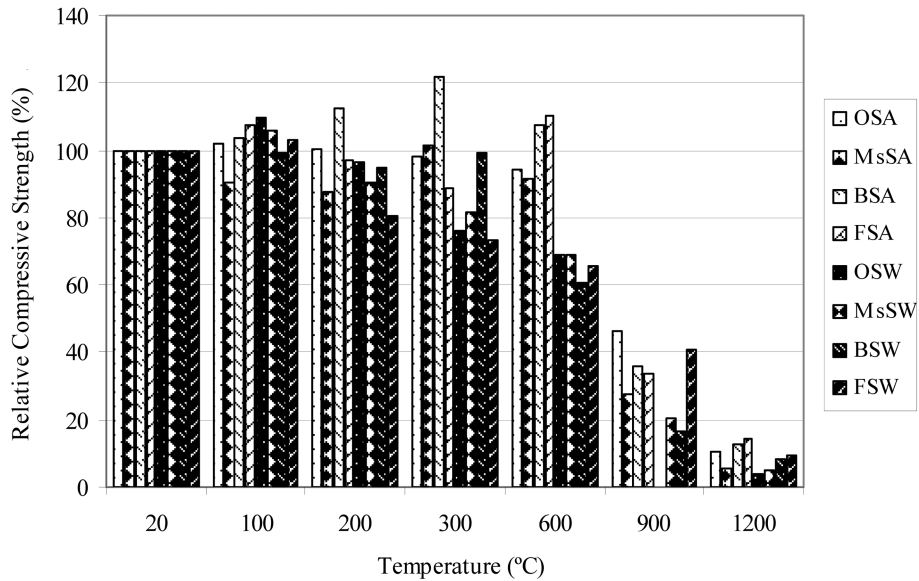


Fig. 6 The relation between the relative compressive strength and temperature of the mortars with siliceous sand

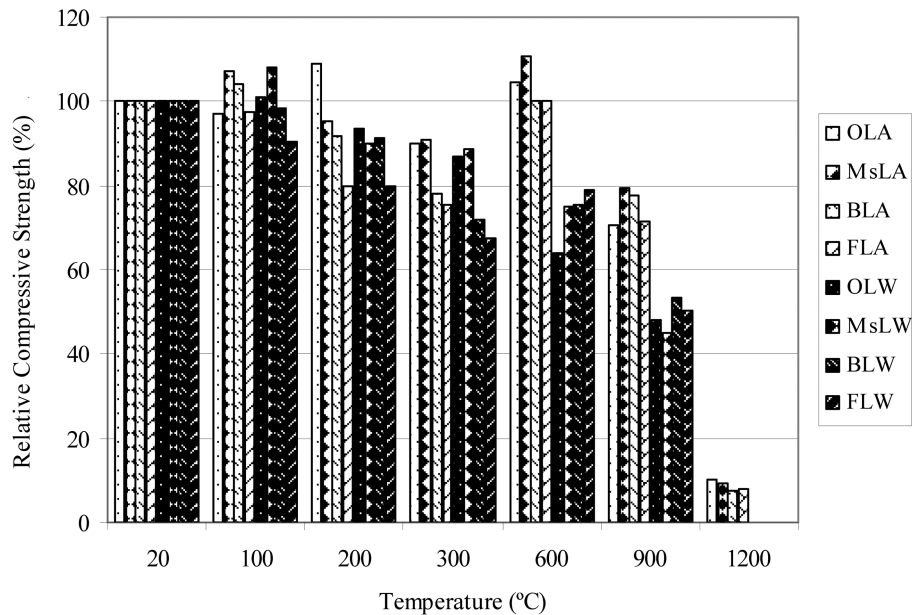


Fig. 7 The relation between the relative compressive strength and temperature of the mortars with calcareous sand

the rehydration of the dehydrated components of the cement paste causes changes in volume, cracks occur and the concrete turns into a porous structure (Dias *et al.* 1990, Andrade *et al.* 2003). The use of mineral admixtures in the mortars exposed to high temperature did not significantly influence the rate of strength loss in comparison to the mortars without mineral admixtures. The mortars made with calcareous aggregates have shown better performance (especially at 900°C) than mortars made

with siliceous aggregates (Figs. 6 and 7). This occurs because the effect of aggregates on the concrete behavior at elevated temperature depends on their mineralogical compositions.

Before the high-temperature effect, as seen in Table 4, the hue component of all samples is yellow, lightness is medium dark and chroma is very weak. For all groups, when the temperature

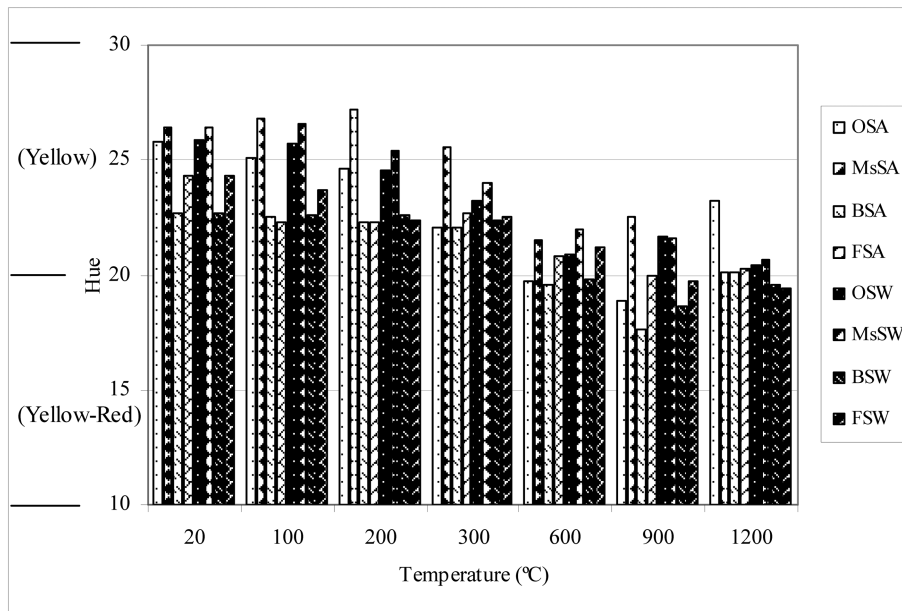


Fig. 8 The relation between the color change (hue) and temperature of the mortars with siliceous sand

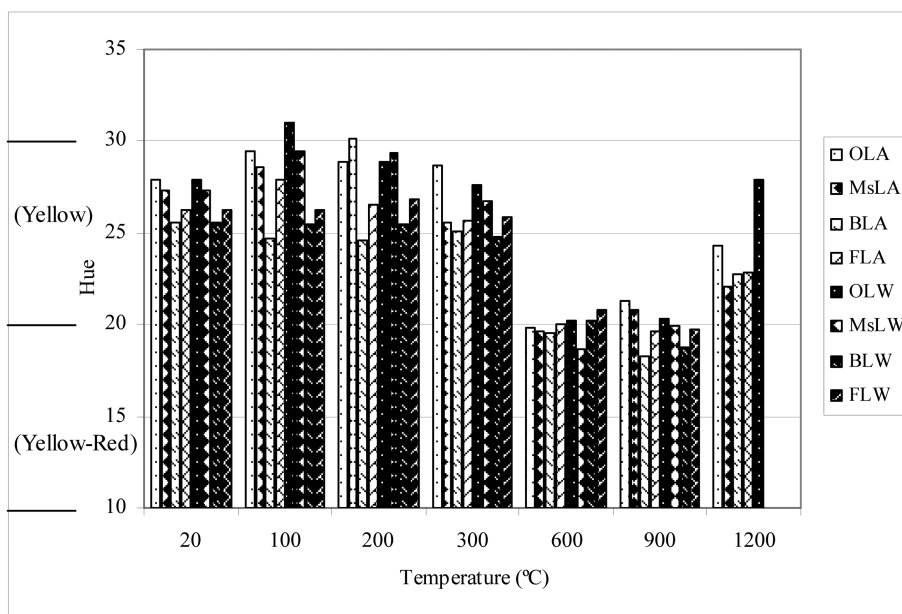


Fig. 9 The relation between the color change (hue) and temperature of the mortars with calcareous sand

increased from 20 to 300°C, the hue of color changed a little from yellow into greenish yellow, at 300°C again, yellow, when increased from 300 to 1200°C, it became reddish yellow (Figs. 8 and 9). The lightness component of the color shows difference for cooling regime. Specimens cooled in air lighter than specimens cooled in water at 600°C and above (Figs. 10 and 11). When the chroma component is examined the change is very low in all groups from 20 to 600°C. But bigger increase occurs at 900 and 1200°C (Figs. 12 and 13) especially at mortars with siliceous aggregate.

In this study to make accurate prediction of the change in compressive strength, the NN model

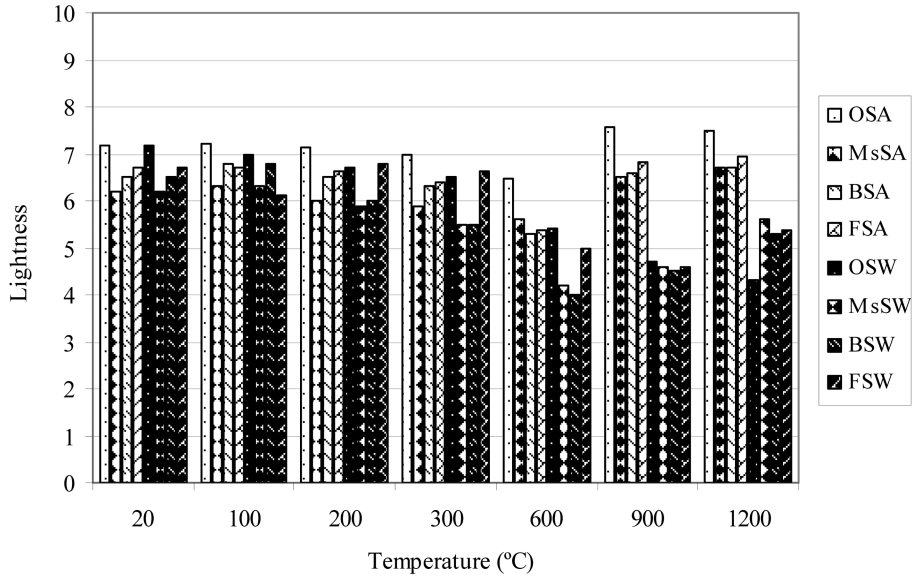


Fig. 10 The relation between the lightness and temperature of the mortars with siliceous sand

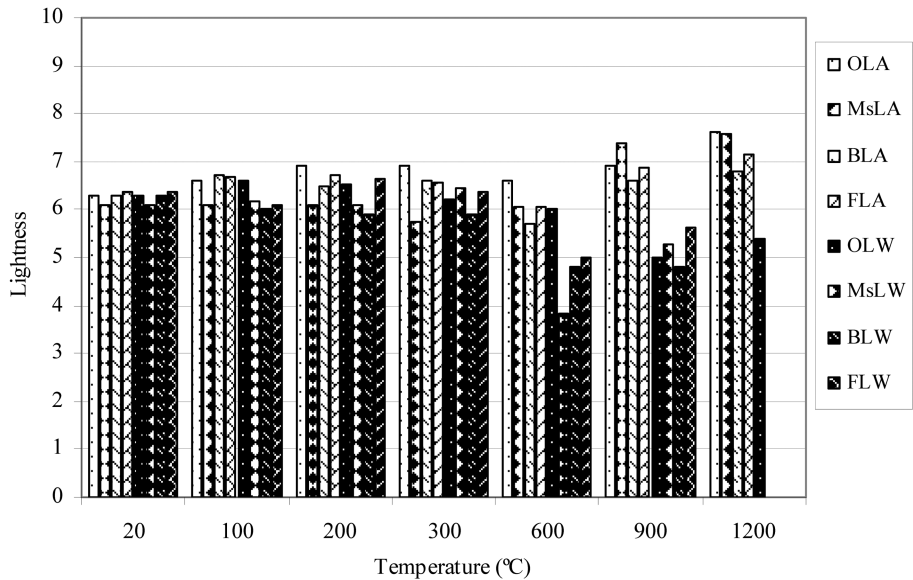


Fig. 11 The relation between the lightness and temperature of the mortars with calcareous sand

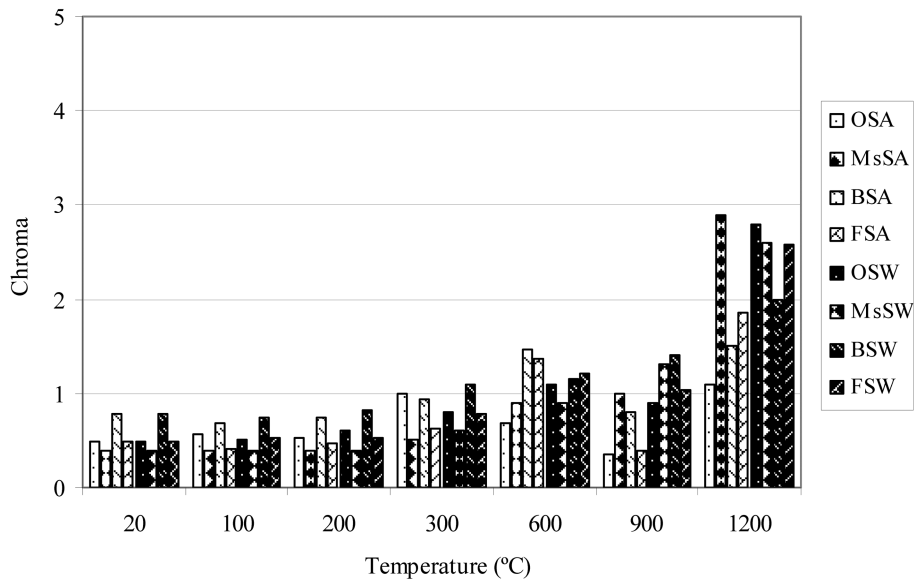


Fig. 12 The relation between the color change (chroma) and temperature of the mortars with siliceous sand

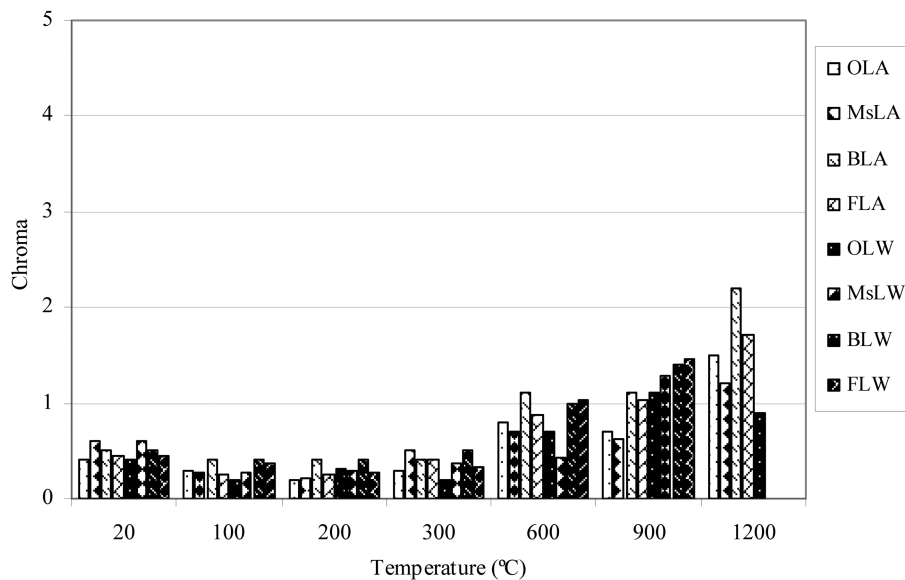


Fig. 13 The relation between the color change (chroma) and temperature of the mortars with calcareous sand

which establishes the non-linear relationship among the three components of color, ultrasonic pulse velocity and the compressive strength of concrete has been applied. Average EPE_{CS} for the 19 testing cases was calculated as 8.94%, while it was 10.48% for the training set (77 cases). Thus, the WE was found to be 9.72%. Fig. 16 shows the error on the estimated compressive strength vs. actual compressive strength for the nineteen testing samples. The last column in Table 6 (Y_{NN}) also shows the estimated compression strength for the training and testing samples. A systematic study

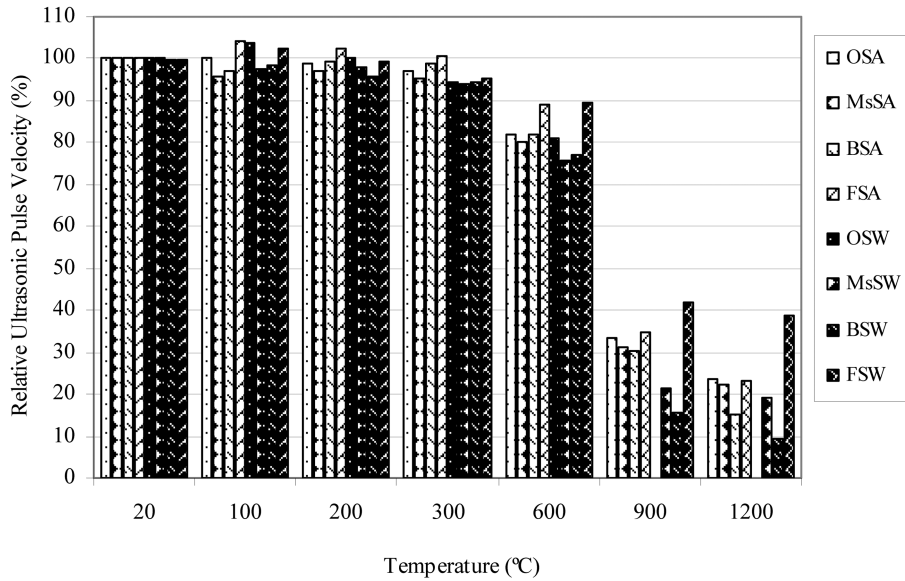


Fig. 14 The relation between the ultrasonic pulse velocity and temperature of the mortars with siliceous sand

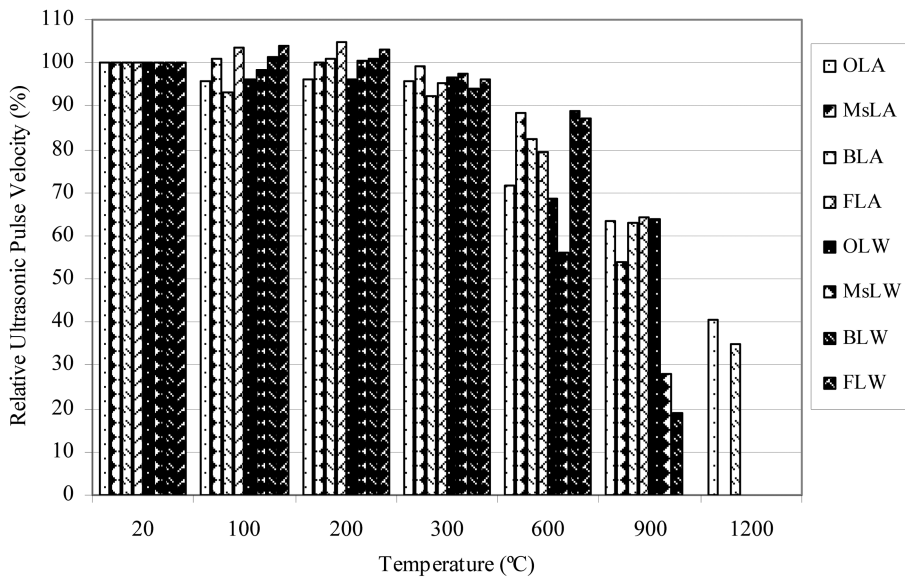


Fig. 15 The relation between the ultrasonic pulse velocity and temperature of the mortars with calcareous sand

was also carried out to determine the effect of the number of hidden layers and PEs (Table 7). For this purpose, the number of PEs is selected as 4, 6, 8, 10, 12, and 20 for two different NN models having one and two hidden layers, respectively. As can be seen from Table 7, as the number of PEs increase, the error for the training cases as well as testing cases tend to decrease for NN models having only one hidden layer. As the number of hidden layers increase, the error for the testing cases increases significantly. Table 7 shows the NN model used in this study having one hidden

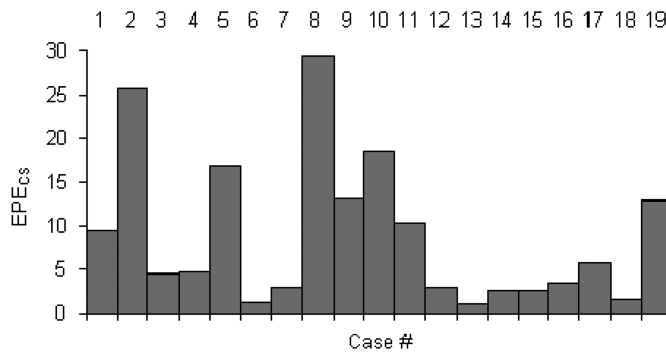


Fig. 16 Error on the estimated compression strength vs. actual compression strength for the nineteen testing samples

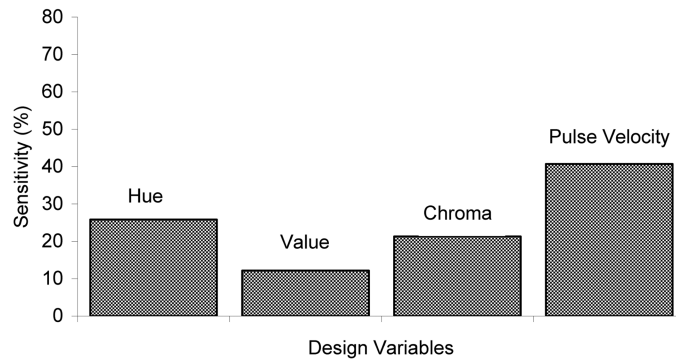


Fig. 17 Sensitivity analyses results

Table 7 Effect of number of hidden layers and PEs

Number of hidden layers	Number of PEs	Error for the training case (%)	Error for the testing case (%)	WE (%)
1	4	10.48	8.94	9.72
	6	12.04	13.05	12.55
	8	9.75	12.39	11.07
	10	9.67	12.43	11.05
	12	10.96	10.61	10.79
	20	9.27	12.11	10.69
2	4	13.12	11.03	12.08
	6	9.64	11.37	10.51
	8	9.89	13.37	11.63
	10	7.11	12.99	10.05
	12	7.27	12.61	9.94
	20	5.51	14.15	9.83

layer and 4 PEs gives the smallest WE and the error for the training and testing cases for this model are close the each other. It is noteworthy that the error for the training cases is the smallest in the NN model having 2 hidden layers and 20 PEs, however it is the highest for the testing cases in the

same NN model (Table 7). In one of our previous studies (Yuzer *et al.* 2007), high temperature effect on concrete that is produced with siliceous aggregate and different pozzolan such as silica fume, fly ash and slag was investigated using a NN model. A relation was established between color components, ultrasonic pulse velocity, and residual compressive strength. When the actual and predicted residual compressive strength were compared the results showed 96.47% of average accuracy for testing cases.

After the NN model was trained, a sensitivity analysis was performed to explore the cause and effect relationship between the input and output parameters on the model. Sensitivity analysis provides valuable information as to which input parameters have the most significant effect on the NN model. This gives the user the option of eliminating the insignificant input channels from the network reducing the size of the network. This would reduce the complexity and the training times. During the analysis, the network weights are not affected, because the network training is disabled. The inputs to the network are temporarily increased and the corresponding change in the output is reported as a percentage summing to 100% in total (Neuro Solutions 2003). The pulse velocity was found to be the most effective parameter on compressive strength with 40.7%, while lightness was found to be the least significant parameter with 12.16%. The effects of hue and chroma were 25.83% and 21.31%, respectively (Fig. 17).

6. Conclusions

A NN model was constructed to develop and test the compressive strength of mortar by using the four input parameters color components (hue, lightness and chroma) and ultrasonic pulse velocity. The data of 77 cases were used to train the NN model. The testing of the NN model was done by the data from 19 testing cases. The average accuracy was found to be 90.3%. The results showed that providing accurate estimates of compressive strength by using the four design parameters were possible using the approach adopted in this study. It should also be noted that the small attributes, which might be provided by the other parameters, may enhance the NN's prediction capability, i.e. the more the number of input parameters, the higher the accuracy. The NN model constructed in this paper can predict well the compressive strength of concrete with given color parameters and pulse velocity if they vary in the range used in this study.

It is recommended that the color change may give an indication of both the temperature to which concrete has been exposed, and the loss of compressive strength. The color change on the surface of the concrete structure exposed to high temperature may be used as a non-destructive testing method to evaluate the residual properties of the concrete.

Acknowledgements

The authors would like to express their thanks Yildiz Technical University Research Foundation and the Scientific Research Council of Turkey (TUBITAK) for their financial support.

References

- Akman, M.S. and Güner, A. (1984), "The applicability of sonreb method on damaged concrete", *Matériaux et Constructions*, **17**(99), 195-200.
- Andrade, C., Alonso, C. and Khoury, G.A. (2003), "Relating microstructure to properties", International Centre for Mechanical Sciences, *Course on Effect of Heat on Concrete*, Udine/Italy.
- ASTM D 1535-08 (2008), *Standard practice for specifying color by the Munsell system*.
- Bilim, C., Atis, C.D., Yanyildizi, H. and Karahan, O. (2009), "Predicting the compressive strength of ground granulated blast furnace slag concrete using artificial network", *Adv. Eng. Softw.*, **40**(5), 334-340.
- Chiang, C.H. and Yang, C.C. (2005), "Artificial neural networks in prediction of concrete strength reduction due to high temperature", *ACI Mater. J.*, **102**(2), 93-102.
- Dias, W.P.S., Khoury, G.A. and Sullivan, P.J.E. (1990), "Mechanical properties of hardened cement paste exposed to temperatures up to 700 C (1292 F)", *ACI Mater. J.*, **87**(2), 160-166.
- Flood, I. (1989), "A neural network approach to the sequencing of construction tasks", *Proceedings of the Sixth International Symposium on Automation and Robotics in Construction*, Austin, Texas, Construction Industry Institute, 204-211.
- Garret, J.H., Gunaratham, D.J. and Ivezic, N. (1997), *Artificial neural networks for civil engineers: fundamentals and applications*, Kartam N, Flood I, editors. ASCE, 1-17.
- Gunaydin, H.M. and Dogan, S.Z. (2004), "A neural network approach for early cost estimation of structural systems of buildings", *Int. J. Project Manage.*, **22**, 595-602.
- Haykin, S. (1994), *Neural networks: a comprehensive foundation*, Macmillan College Publishing Company, Inc, NJ-USA.
- Hegazy, T. and Ayed, A. (1998), "Neural network model for parametric cost estimation of highway projects", *J. Constr. Eng. Manage.*, **124**(3), 210-218.
- Luke, J.T. (1996), *The Munsell Color System: A Language for color*, Fairchild Publications.
- Luo, H.L. and Lin, D.F. (2007), "Study the surface color of sewage mortar at high temperature", *Constr. Build. Mater.*, **21**(1), 90-97.
- Neuro Solutions (2003), *Neurodimension Inc.*, Version 4.24.
- Neville, A.M. (2000), *Properties of Concrete*, Fourth Edition, Longman Scientific and Technical, 359-411.
- Parichatprecha, R. and Nimityongskul, P. (2009), "Analysis of durability of high performance concrete using artificial neural networks", *Constr. Build. Mater.*, **23**(2), 910-917.
- Rafiq, M.Y., Bugmann, G. and Easterbrook, D.J. (2001), "Neural network design for engineering applications", *Comp. Struct.*, **79**(17), 1541-1552.
- Saridemir, M. (2009), "Prediction of compressive strength of concretes containing metakaolin and silica fume by artificial networks", *Adv. Eng. Softw.*, **40**(5), 350-355.
- Shackelford, J.F. (2005), *Introduction to materials science for engineers*, Sixth Edition, Pearson Education Inc.
- Short, N.R., Purkiss, J.A. and Guise, S.E. (2001), "Assessment of fire damaged concrete using colour image analysis", *Constr. Build. Mater.*, **15**(1), 9-15.
- TS EN 196-1 (2002), *Methods of testing cement-Part 1: Determination of strength*.
- Yeung, W.T. and Smith, J.W. (2005), "Damage detection in bridges using neural networks for pattern recognition of vibration signatures", *Eng. Struct.*, **27**(5), 685-698.
- Yuzer, N., Akbas, B. and Kizilkanat, A.B. (2007), "Predicting the compressive strength of concrete exposed to high temperatures with a neural network model", *TCMB 3rd International Symposium Sustainability in Cement and Concrete*, Istanbul, Turkey, 455-464.
- Yuzer, N. and Kizilkanat, A.B. (2008), "Compressive strength-color change relationship in mortars subjected to high temperatures", *Teknik Dergi*, **19**(2), 4381-4392.
- Wang, H.Y. (2008), "Effect of elevated temperatures on properties and color intensities of fly ash mortar", *Comput. Concrete*, **5**(2), 89-100.
- Zhao, Z. (2006), "Steel columns under fire-A neural network based strength model", *Adv. Eng. Softw.*, **37**(2), 97-105.

Notations

$Amplitude(i)$	= normalization coefficient for processing element i
$Data(i)$	= neural network data for processing element i
EPE_{CS}	= compressive strength percentage error
$f(x_i)$	= hyperbolic tangent function
$lowerlimit$	= -1
$max(i)$	= maximum value within the input processing element i
$min(i)$	= minimum value within the input processing element i
MSE	= mean square error
n	= number of samples
$Normalized\ Data(i)$	= normalized data for processing element i
$Offset(i)$	= normalization coefficient for processing element i
u_i	= output of a processing element
$upperlimit$	= 1
x_i	= neural network model output related to sample i
X_i	= target output related to sample i
w_{ij}	= synaptic weights associated with processing element PE i
$WE(\%)$	= overall performance of the neural network model
β	= parameter that controls the slope of $f(x_i)$
θ_i	= threshold value of the processing element
$\phi(.)$	= activation (or transformation) function